

Quasicycles in the stochastic hybrid Morris-Lecar neural model

Heather A. Brooks and Paul C. Bressloff*

Department of Mathematics, University of Utah, 155 South 1400 East, Salt Lake City, Utah 84112, USA

(Received 2 February 2015; published 6 July 2015)

Intrinsic noise arising from the stochastic opening and closing of voltage-gated ion channels has been shown experimentally and mathematically to have important effects on a neuron's function. Study of classical neuron models with stochastic ion channels is becoming increasingly important, especially in understanding a cell's ability to produce subthreshold oscillations and to respond to weak periodic stimuli. While it is known that stochastic models can produce oscillations (quasicycles) in parameter regimes where the corresponding deterministic model has only a stable fixed point, little analytical work has been done to explore these connections within the context of channel noise. Using a stochastic hybrid Morris-Lecar (ML) model, we combine a system-size expansion in K^+ and a quasi-steady-state (QSS) approximation in persistent Na^+ in order to derive an effective Langevin equation that preserves the low-dimensional (planar) structure of the underlying deterministic ML model. (The QSS analysis exploits the fact that persistent Na^+ channels are fast.) By calculating the corresponding power spectrum, we determine analytically how noise significantly extends the parameter regime in which subthreshold oscillations occur.

DOI: [10.1103/PhysRevE.92.012704](https://doi.org/10.1103/PhysRevE.92.012704)

PACS number(s): 87.19.lc, 87.10.Mn, 05.40.—a

I. INTRODUCTION

Noise has emerged as a key component of a wide range of biological systems [1]. In the particular case of neuroscience, noise is present at all levels, yet neural networks are still able to perform complex computations reliably [2]. The most dominant source of intrinsic noise in neurons is ion channel noise [3,4]. The membrane potential of a neuron changes as ions such as Na^+ and K^+ pass in and out of the cell through voltage-dependent channels within the membrane and the opening and closing of the channels is stochastic due to thermal fluctuations [5]. In classical approaches, the number of ion channels is assumed to be very large and thus the fluctuations in membrane potential from individual stochastic channels is ignored in favor of a deterministic average. More recent work has questioned this assumption. It has been shown that channel noise indeed produces membrane potential fluctuations that are large enough to affect action potential timing [6–11] and increase the range of spiking behavior exhibited in some neural populations [3], with the effects of channel noise increasing dramatically as neurons become smaller. However, even when large numbers of stochastic ion channels are present in a neuron, fluctuations can become critical near the action potential threshold [2,12]. In addition, sodium channel noise places structural limits on neural anatomy [13], since in the case of very small neurons, significant channel noise would disrupt signal transmission [14].

Ion channel noise has also been implicated in subthreshold membrane potential oscillations (STOs). These are observed in a variety of neural cell types: stellate cells in the entorhinal cortex, hippocampal cells, and mitral cells in the olfactory bulb, to name a few. Intrinsic ion currents are sufficient to produce oscillatory activity [15]. Tetrodotoxin blocks STOs, implicating a persistent Na^+ current in the generation of oscillatory activity [16–20]. Using the dynamic clamp technique, it has been shown that stochastic flicker of these persistent

sodium channels is crucial for subthreshold oscillations and phase locking to weak periodic stimuli in entorhinal spiny stellate cells [13]. Hyperpolarization is due to a noninactivating outward current, for example, a tetraethylammonium-sensitive M current in layer- V pyramidal cells [20]. In addition to the phase locking of periodic stimuli, it has been shown experimentally and theoretically that noise can enhance weak signal transduction in sensory neurons via tuning intrinsic subthreshold oscillations [21]. White *et al.* [18] showed that the presence of channel noise alters the dynamical behavior of a medial entorhinal cortical cell model; in particular, subthreshold oscillations are most easily generated for intermediate noise levels. In these cells, it is predicted that there are only on the order of 1000–5000 persistent Na^+ channels, a surprisingly small number that does not match the assumptions of classical deterministic neuron model approaches.

Deterministic conductance-based models of a single neuron such as the Hodgkin-Huxley model have been widely used to understand the dynamical mechanisms underlying membrane excitability [22]. These models assume a large population of ion channels so that their effect on membrane conductance can be averaged. As a result, the average fraction of open ion channels modulates the effective ion conductance, which in turn depends on voltage. It is often convenient to consider a simplified planar model of a neuron, which tracks the membrane voltage v and a recovery variable w that represents the fraction of open potassium channels. The advantage of a two-dimensional model is that one can use phase-plane analysis to develop a geometric picture of neuronal spiking. One well-known example is the Morris-Lecar (ML) model [23]. Although this model was originally developed to model Ca^{2+} spikes in mollusks, it has been widely used to study both type-I and type-II forms of neural excitability for Na^+ spikes [22] since it exhibits many of the same bifurcation scenarios as more complex models. The ML model has also been used to investigate STOs due to persistent Na^+ currents [24].

Another advantage of the ML model is that it is straightforward to incorporate intrinsic channel noise [25–27]. In order to

*bressloff@math.utah.edu

capture the fluctuations in membrane potential from stochastic switching in voltage-gated ion channels, the resulting model includes both discrete jump processes (to represent the opening and closing of ion channels) and a continuous-time piecewise process (to represent the membrane potential). This is an example of a stochastic hybrid system with piecewise deterministic dynamics. There has been much recent interest in such systems, within the context of both conductance-based models and gene and biochemical networks [1].

In this paper we use a stochastic hybrid ML model of a persistent (noninactivating) sodium current and a slower outward potassium current to investigate analytically the role of channel noise in the generation of STOs. Previous computational studies have shown how channel noise can significantly extend the parameter regime over which STOs occur [18,28]. We show that such a phenomenon can be analyzed in terms of the emergence of so-called quasicycles below a supercritical Hopf bifurcation point of the corresponding deterministic model. The emergence of quasicycles in a stochastic model—periodic oscillations that arise outside the limit cycle regime of a deterministic system—has been studied in various biological applications (see [29–33]). In some cases, such as calcium oscillations, the addition of noise serves to expand the range of parameter values for which limit cycle behavior is observed [29]; it is also possible in some reaction networks to induce oscillations where there are no limit cycles anywhere in the parameter space of the deterministic system [30].

In addition to providing an analytical framework for understanding noise-induced STOs, we introduce a mathematical approach to study quasicycles in stochastic hybrid systems. Typically, the emergence of quasicycles in a jump Markov process is handled by carrying out a system-size expansion of the underlying master equation. This generates a Fokker-Planck (FP) equation, whose corresponding Langevin equation can be linearized about the fixed point solution of the deterministic system below the Hopf-bifurcation point. If the resulting power spectrum exhibits a significant peak at a nonzero frequency, then this indicates the existence of a quasicycle. In the case of the stochastic ML model, one could carry out a double system-size expansion with respect to the total number N of Na^+ channels and the total number M of K^+ channels. However, this would lead to a multivariate Langevin equation in three stochastic variables: the voltage v , the fraction w of open K^+ channels, and the fraction A of open Na^+ channels. Instead, we would like to preserve the low-dimensional (planar) structure of the ML model by deriving a Langevin equation for v and w alone.¹ We show how

this can be achieved by exploiting the fact that the opening and closing of the persistent Na^+ channels is much faster than the dynamics of the voltage and the K^+ channels. We thus combine a quasi-steady-state (QSS) analysis of the Na^+ dynamics and a system-size expansion of the K^+ dynamics to derive a Langevin equation for the pair (v, w) and relate the existence of noise-induced STOs to the power spectrum of the resulting stochastic voltage. We briefly review the deterministic ML model in Sec. II, with parameter values chosen so that the model supports subthreshold oscillations via a supercritical Hopf bifurcation, rather than the more familiar spiking via a subcritical Hopf bifurcation. The stochastic version of the ML model is introduced in Sec. III, which is then systematically reduced by carrying out a system-size expansion with respect to K^+ (Sec. IV) and a QSS approximation with respect to Na^+ (Sec. V). The emergence of quasicycles (noise-induced STOs) is then established in Sec. VI.

II. DETERMINISTIC MODEL

A version of the deterministic Morris-Lecar model [23] has previously been used to understand the initiation and behavior of STOs [24]. The model consists of a persistent sodium current Na^+ , a slow potassium current K^+ , a leak current L , and an applied current I_{app} . For simplicity, each ion channel is treated as a two-state system that switches between an open and a closed state; the more detailed subunit structure of ion channels is neglected [11,25]. The membrane voltage v evolves as

$$\begin{aligned} \frac{dv}{dt} &= a_{\infty}(v)f_{\text{Na}}(v) + wf_{\text{K}}(v) + f_L(v) + I_{\text{app}}, \\ \frac{dw}{dt} &= (1-w)\alpha_{\text{K}}(v) - w\beta_{\text{K}}, \end{aligned} \quad (2.1)$$

where w is the K^+ gating variable. It is assumed that Na^+ channels are in quasi-steady-state $a_{\infty}(v)$, thus eliminating Na^+ as a variable. For $i = \text{K}, \text{Na}, L$, let $f_i = g_i(V_i - v)$, where g_i are ion conductances and V_i are reversal potentials. Opening and closing rates of ion channels depending only on membrane potential v are represented by α and β , respectively, so that

$$a_{\infty}(v) = \frac{\alpha_{\text{Na}}(v)}{\alpha_{\text{Na}}(v) + \beta_{\text{Na}}(v)}. \quad (2.2)$$

For concreteness, take

$$\alpha_i(v) = \beta_i \exp\left(\frac{v - v_{i,1}}{v_{i,2}}\right), \quad i = \text{K}, \text{Na}, \quad (2.3)$$

with β_i , $v_{i,1}$, and $v_{i,2}$ constant. Parameters are chosen (see Table I) such that there is no well-defined threshold above which an action potential is generated; rather, stable small-amplitude oscillations arise for a sufficient value of applied current (this appears in the model as a supercritical Hopf bifurcation). This corresponds well to the observed behavior of STOs and is not meant to function as a traditional spiking neuron model. Limit cycles in a traditional spiking model

¹One motivation for preserving the planar structure of the ML model is that we would ultimately like to incorporate our theory of subthreshold oscillations into a model of spontaneous action potentials for an excitable neuron. This would require including a population of nonpersistent Na^+ ion channels along the lines of [27]. The analysis of the resulting escape problem becomes almost intractable beyond planar systems, so it is preferable to carry out a slow-fast analysis rather than a system-size expansion with respect to the two classes of Na^+ channels. The advantage of maintaining a low-dimensional Langevin equation by performing a slow-fast

analysis rather than a system-size expansion also becomes significant when the complexity of the fast ion channels increases (see also Sec. VII).

TABLE I. Model parameters to generate subthreshold oscillations via a supercritical Hopf bifurcation. Note that we assume capacitance $C = 1 \mu\text{F}$.

Sodium					Leak		Potassium				
g_{Na}	V_{Na}	β_{Na}	$v_{n,1}$	$v_{n,2}$	g_L	V_L	g_K	V_K	β_K	$v_{k,1}$	$v_{k,2}$
4.4 mS	55 mV	100 ms ⁻¹	-1.2 mV	18 mV	2 mS	-60 mV	8 mS	-84 mV	0.35 ms ⁻¹	2 mV	30 mV

often appear via a subcritical Hopf bifurcation. We do not provide further analysis for the subcritical Hopf case in this work; however, in the presence of noise, a transition to the oscillatory state has also been observed to shift in the vicinity of a subcritical Hopf bifurcation (see, for example, [34]). Thus, it is not unreasonable to expect that similar results may hold.

By evaluating the eigenvalues of the Jacobian of Eq. (2.1), it is straightforward to show that there is a unique steady state (v^*, w^*) , which is linearly stable for $I_{\text{app}} < I_{\text{app}}^*$ [22]. At I_{app}^* a supercritical Hopf bifurcation occurs; (v^*, w^*) becomes unstable and a stable limit cycle emerges (see Fig. 1). Figure 2 shows the phase plane of the deterministic system; here one can see how oscillations arise in the membrane potential $v(t)$ as the applied current is increased.

III. STOCHASTIC MODEL

The deterministic ML model holds under the assumption that the number of ion channels is very large, thus the ion channel activation can be approximated by the average ionic currents. However, it is known that channel noise does affect membrane potential fluctuations (and thus neural function) and the number of persistent Na⁺ channels is on the order of 10³ [3,18]. In order to account for ion channel fluctuations, we consider a stochastic version of the Morris-Lecar model [25–27], with M K⁺ channels and N Na⁺ channels. Let $m(t)$ denote the number of open K⁺ channels and $n(t)$ the number of open Na⁺ channels at time t . Since it follows that the number of closed channels at time t is $M - m$ and $N - n$, respectively, there is no need to also track the number of closed channels. Then, for $m(t) = m$ and $n(t) = n$, the voltage evolves according to the equation

$$\frac{dv}{dt} = \frac{n}{N} f_{\text{Na}}(v) + \frac{m}{M} f_{\text{K}}(v) + f_L(v) + I_{\text{app}}. \quad (3.1)$$

$$\begin{aligned} \frac{\partial P}{\partial t} = & -\frac{\partial}{\partial v} \left[\left(\frac{n}{N} f_{\text{Na}}(v) + \frac{m}{M} f_{\text{K}}(v) + f_L(v) + I_{\text{app}} \right) P(v, n, m, t) \right] \\ & + \frac{1}{\epsilon} [\omega_n^+(v, n-1)P(v, n-1, m, t) + \omega_n^-(v, n+1)P(v, n+1, m, t)] - \frac{1}{\epsilon} [\omega_n^+(v, n) + \omega_n^-(v, n)]P(v, n, m, t) \\ & + [\omega_m^+(v, m-1)P(v, n, m-1, t) + \omega_m^-(v, m+1)P(v, n, m+1, t)] - [\omega_m^+(v, m) + \omega_m^-(v, m)]P(v, n, m, t). \end{aligned} \quad (3.4)$$

The first line on the right-hand side represents the piecewise deterministic dynamics of v , whereas the second and third lines represent the stochastic opening and closing of Na⁺ and K⁺ ion channels, respectively. It is not possible to obtain exact solutions of the CK equation, so some sort of approximation is needed.

We assume that the state transitions of the ion channels are given by a discrete Markov process, that is, ion channels are memoryless and the probability per unit time of changing states depends only on the current state, not on any past events (including the amount of time spent in the current state). In this case, sodium and potassium channels switch between open O and closed C states as follows:

$$C \xrightleftharpoons[\beta_{\text{Na}}/\epsilon]{\alpha_{\text{Na}}(v)/\epsilon} O, \quad C \xrightleftharpoons[\beta_K]{\alpha_K(v)} O. \quad (3.2)$$

The opening and closing of these channels is a birth-death process, where n and m evolve according to

$$\begin{aligned} n &\rightarrow n-1, & \omega_n^- &= n\beta_{\text{Na}}, \\ n &\rightarrow n+1, & \omega_n^+ &= (N-n)\alpha_{\text{Na}}(v), \\ m &\rightarrow m-1, & \omega_m^- &= m\beta_K, \\ m &\rightarrow m+1, & \omega_m^+ &= (M-m)\alpha_K(v). \end{aligned} \quad (3.3)$$

The above model is an example of a stochastic hybrid system based on a piecewise deterministic process. That is, the transition rates depend on v , with the latter coupled to the associated jump Markov process according to Eq. (3.1), which is only defined between jumps, during which $v(t)$ evolves deterministically. Furthermore, we assume that Na⁺ channels open and close much faster than K⁺ channels. We define $\epsilon = O(10^{-2})$ as a time scale variable for Na⁺. Define $P(v, n, m, t)dv = \text{Prob}[n(t) = n; m(t) = m; v \leq v(t) \leq v + dv]$ at time t , given initial conditions $v(0) = v_0$, $m(0) = m_0$, and $n(0) = n_0$. Dropping the explicit dependence on initial conditions, this probability density will then satisfy the differential Chapman-Kolmogorov (CK) equation

IV. SYSTEM-SIZE EXPANSION OF POTASSIUM

Suppose that M is large (but finite). Then it is possible to carry out a perturbation expansion in terms of the system size M^{-1} , which allows us to approximate the potassium dynamics as a continuous process [1,35,36]. The system-size expansion is a standard technique in stochastic processes

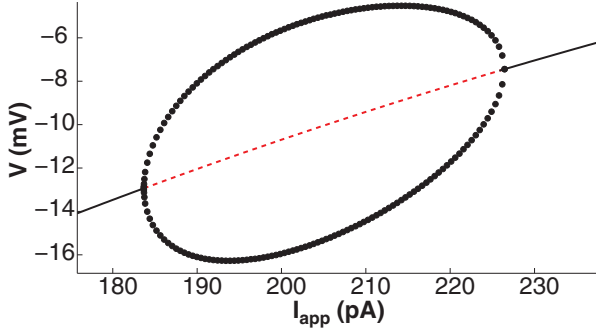


FIG. 1. (Color online) Bifurcation diagram of the deterministic model. As I_{app} is increased, the system undergoes a supercritical Hopf bifurcation H at $I_{\text{app}}^* = 183$, which leads to the generation of stable oscillations. The maximum and minimum values of oscillations are plotted as solid (black) curves. Oscillations disappear via another supercritical Hopf bifurcation.

that allows us to describe fluctuations about the deterministic theory via second-order terms in the expansion. It was first introduced within the context of stochastic ion channels by Fox and Lu [6] and further developed by Chow and White [7]. (More precisely, these authors assumed that the stochastic dynamics of a large population of identical ion channels can be approximated by a Gaussian process and then calculated the mean and variance based on single-channel properties.) First we introduce rescaled variables

$$w = \frac{m}{M}, \quad M\Omega_{\pm}(w) = \omega_m^{\pm}(Mw) \quad (4.1)$$

and set $p_n(v, w, t) = P(v, n, Mw, t)$. In order for the system-size expansion to be valid, it is important to note that the

transition rates ω_m^{\pm} scale as specified. It is straightforward to check that this condition is satisfied for our model. Thus we rewrite Eq. (3.4) as

$$\begin{aligned} \frac{\partial p_n}{\partial t} = & -\frac{\partial}{\partial v} \{I_n(v, w)p_n(v, w, t)\} + \frac{1}{\epsilon} [\omega_n^+(v, n-1) \\ & \times p_{n-1}(v, w, t) + \omega_n^-(v, n+1)p_{n+1}(v, w, t)] \\ & - \frac{1}{\epsilon} \{[\omega_n^+(v, n) + \omega_n^-(v, n)]p_n(v, w, t)\} - M\{[\Omega_+(v, w) \\ & + \Omega_-(v, w)]p_n(v, w, t)\} \\ & + M \left\{ \left[\Omega_+ \left(v, w - \frac{1}{M} \right) p_n \left(v, w - \frac{1}{M}, t \right) \right. \right. \\ & \left. \left. + \Omega_- \left(v, w + \frac{1}{M} \right) p_n \left(v, w + \frac{1}{M}, t \right) \right] \right\}, \quad (4.2) \end{aligned}$$

where

$$I_n(v, w, t) = wf_K(v) + \frac{n}{N} f_{\text{Na}}(v) + f_L(v) + I_{\text{app}}. \quad (4.3)$$

Note that for M sufficiently large, w can be treated as a continuous variable, where $0 \leq w \leq 1$. Taylor expanding in $1/M$ to $O(1/M)$ yields

$$\begin{aligned} \frac{\partial p_n}{\partial t} = & -\frac{\partial}{\partial v} [I_n(v, w)p_n] - \frac{\partial}{\partial w} [B_-(v, w)p_n] \\ & + \frac{1}{2M} \frac{\partial^2}{\partial w^2} [B_+(v, w)p_n] + \frac{1}{\epsilon} [\omega_n^+(v, n-1)p_{n-1} \\ & + \omega_n^-(v, n+1)p_{n+1}] - \frac{1}{\epsilon} \{[\omega_n^+(v, n) + \omega_n^-(v, n)]p_n\}, \quad (4.4) \end{aligned}$$

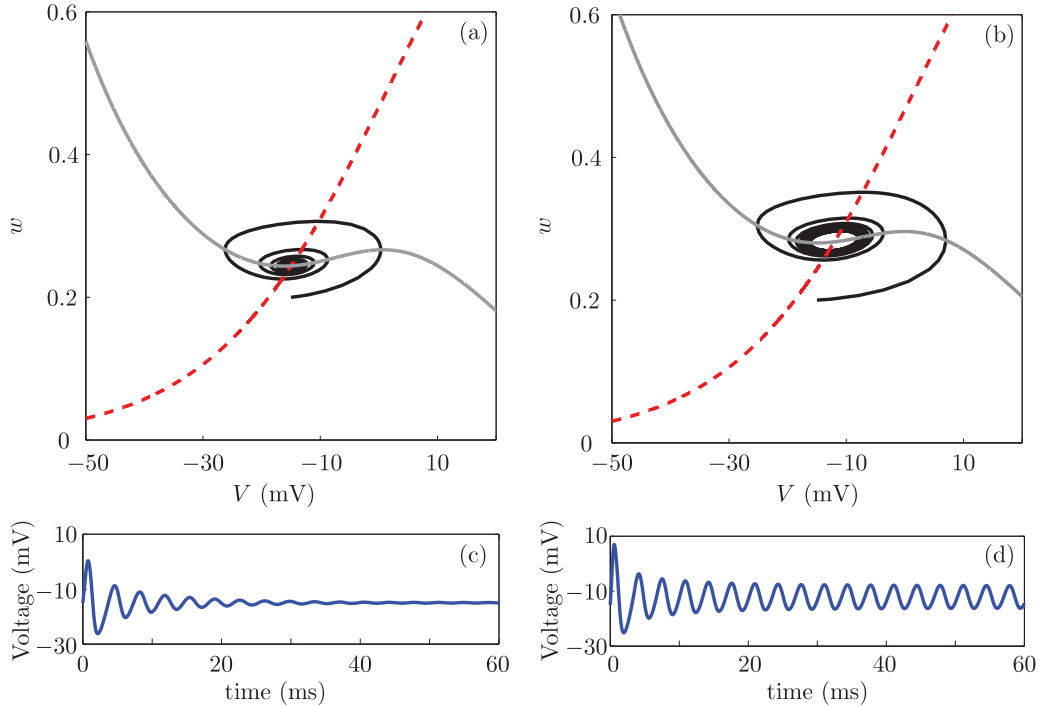


FIG. 2. (Color online) Phase plane diagrams of the deterministic model for (a) $I_{\text{app}} = 170$ pA (below the Hopf bifurcation point) and (b) $I_{\text{app}} = 190$ pA (above the Hopf bifurcation point). The dashed (red) curve is the w nullcline and the solid (gray) curve represents the v nullcline. The intersection of nullclines is the fixed point (v^*, w^*) . (c) and (d) Corresponding voltage time courses.

where

$$B_-(v, w) = \Omega_+ - \Omega_-, \quad B_+(v, w) = \Omega_+ + \Omega_-. \quad (4.5)$$

Note that the system-size expansion has replaced the jump-Markov process for the K^+ channels by a continuous diffusionlike process for the fraction of open K^+ channels. The variance associated with the stochastic K^+ channels scales as $\sigma_K^2 \sim M^{-1}$. One could proceed in a similar fashion for the Na^+ ion channels by carrying out a system-size expansion with respect to N . This would then lead to a multivariate FP equation for the three variables v , w , and a , where a is the fraction of open Na^+ ion channels. Note in particular that the variance associated with the stochastic Na^+ channels would scale as $\sigma_{Na}^2 \sim (\epsilon N)^{-1}$. Since $\epsilon \ll 1$ and $N \ll M$, it immediately follows that the main source of channel noise arises from the persistent Na^+ . In this paper we wish to develop an alternative approximation of the stochastic hybrid system that preserves the planar nature of the deterministic ML model. We will make use of the fact that the Na^+ jump process is much faster than potassium or voltage to perform a QSS approximation, also known as the adiabatic approximation [1,26,35].

V. QUASI-STEADY-STATE DIFFUSION APPROXIMATION OF SODIUM

Let $W_{nj}(v)$ be the voltage-dependent transition matrix for the Na^+ jump process, that is,

$$W_{nj}(v) = \omega_n^+(v, n-1)\delta_{j, n-1} + \omega_n^-(v, n+1)\delta_{j, n+1} - [\omega_n^+(v, n) + \omega_n^-(v, n)]\delta_{j, n}.$$

Rewrite Eq. (4.4) using this transition matrix

$$\begin{aligned} \frac{\partial p_n}{\partial t} = & -\frac{\partial}{\partial v}[I_n(v, w)p_n] - \frac{\partial}{\partial w}[B_-(v, w)p_n] \\ & + \frac{1}{2M} \frac{\partial^2}{\partial w^2}[B_+(v, w)p_n] + \frac{1}{\epsilon} \sum_j W_{nj}(v)p_j. \end{aligned} \quad (5.1)$$

For fixed values of v , the transition matrix $W_{nj}(v)$ is irreducible. By the Perron-Frobenius theorem, W has a simple zero eigenvalue, with all others having a negative real part. This implies that there exists a unique right null vector $\rho_n(v)$ such that $\sum_j W_{nj}(v)\rho_j(v) = 0$. Furthermore, $(1, 1, \dots, 1)^T$ is the left null vector of W , so $\sum_n W_{nj}(v) = 0$ for all n . For fixed v, w , it can be shown that the Markov process for sodium

$$\begin{aligned} \frac{dp_n}{dt} = & \frac{1}{\epsilon} [\omega_n^+(v, n-1)p_{n-1} + \omega_n^-(v, n+1)p_{n+1}] \\ & - \frac{1}{\epsilon} \{[\omega_n^+(v, n) + \omega_n^-(v, n)]p_n\} \end{aligned} \quad (5.2)$$

has a globally attracting steady state $\rho(v, n) = \rho_n$ such that [27]

$$\rho_n = \frac{N!}{n!(N-n)!} \frac{\alpha_{Na}^n \beta_{Na}^{(N-n)}}{(\alpha_{Na} + \beta_{Na})^N}. \quad (5.3)$$

Since Na^+ is fast, there are many open-close transitions in n while the voltage v and w change very little. Thus we expect that the system will converge to the sodium QSS ρ_n , which will be perturbed as v and w evolve. This can be analyzed using a QSS approximation.

First, we decompose the probability density p_n such that

$$p_n(v, w, t) = C(v, w, t)\rho_n(v) + \epsilon x_n(v, w, t), \quad (5.4)$$

where

$$\sum_n p_n(v, w, t) = C(v, w, t), \quad \sum_n x_n(v, w, t) = 0.$$

Substituting Eq. (5.4) into Eq. (5.1), the CK equation now reads

$$\begin{aligned} \rho_n \frac{\partial C}{\partial t} + \epsilon \frac{\partial x_n}{\partial t} = & -\frac{\partial}{\partial v}[C I_n \rho_n] - \epsilon \frac{\partial}{\partial v}[I_n x_n] \\ & + \mathbb{L}_w[\rho_n C + \epsilon x_n] + \sum_j W_{nj} x_j, \end{aligned} \quad (5.5)$$

where

$$\mathbb{L}_w \psi(w) = -\frac{\partial}{\partial w}[B_- \psi(w)] + \frac{1}{2M} \frac{\partial^2}{\partial w^2}[B_+ \psi(w)]. \quad (5.6)$$

Summing both sides over n and setting $\bar{I} = \sum_n I_n \rho_n$ yields

$$\frac{\partial C}{\partial t} = -\frac{\partial C \bar{I}}{\partial v} - \epsilon \frac{\partial \sum_n I_n x_n}{\partial v} + \mathbb{L}_w C. \quad (5.7)$$

We rewrite Eq. (5.5) by using Eq. (5.7) for $\partial C/\partial t$:

$$\begin{aligned} \epsilon \frac{\partial x_n}{\partial t} = & \left(\frac{\partial C \bar{I}}{\partial v} + \epsilon \frac{\partial \sum_n I_n x_n}{\partial v} \right) \rho_n - \frac{\partial C I_n \rho_n}{\partial v} \\ & - \epsilon \frac{\partial I_n x_n}{\partial v} + \epsilon \mathbb{L}_w x_n + \sum_j W_{nj} x_j. \end{aligned} \quad (5.8)$$

Introducing the asymptotic expansion $x \sim x^{(0)} + \epsilon x^{(1)} + \epsilon^2 x^{(2)} + \dots$ and considering only $O(1)$ terms gives

$$\sum_j W_{nj} x_j^{(0)} = -\frac{\partial C \bar{I}}{\partial v} \rho_n + \frac{\partial C I_n \rho_n}{\partial v}. \quad (5.9)$$

From the Fredholm alternative theorem, Eq. (5.9) has a solution of the form

$$x_j^{(0)} = \sum_j W_{jn}^\dagger \left(-\frac{\partial C \bar{I}}{\partial v} \rho_n + \frac{\partial C I_n \rho_n}{\partial v} \right), \quad (5.10)$$

where W^\dagger is the pseudoinverse of W . Using this solution for $x^{(0)}$ as a leading-order approximation for x_n in (5.7) gives the Fokker-Planck equation

$$\begin{aligned} \frac{\partial C}{\partial t} = & -\frac{\partial}{\partial v} \left(\left[\bar{I} - \epsilon \sum_n \left[\bar{I} \frac{\partial}{\partial v} \left(I_n \sum_j W_{jn}^\dagger \rho_n \right) \right. \right. \right. \\ & \left. \left. \left. - I_n \rho_n \frac{\partial}{\partial v} \left(I_n \sum_j W_{jn}^\dagger \right) \right] \right] C \right) - \frac{\partial}{\partial w}[B_- C] \\ & + \frac{1}{2M} \frac{\partial^2 B_+ C}{\partial w^2} + \epsilon \frac{\partial^2}{\partial v^2} \left(\sum_{n,j} W_{jn}^\dagger I_n \rho_n (\bar{I} - I_n) C \right). \end{aligned} \quad (5.11)$$

Letting

$$\mu_1 = \bar{I} - \epsilon \sum_n \left[\bar{I} \frac{\partial}{\partial v} \left(I_n \sum_j W_{jn}^\dagger \rho_n \right) - I_n \rho_n \frac{\partial}{\partial v} \left(I_n \sum_j W_{jn}^\dagger \right) \right], \quad (5.12a)$$

$$\mu_2 = B_-, \quad (5.12b)$$

$$D = \begin{pmatrix} \epsilon \sum_{n,j} W_{jn}^\dagger I_n \rho_n (\bar{I} - I_n) & 0 \\ 0 & B_+ / 2M \end{pmatrix}, \quad (5.12c)$$

we can simplify the Fokker-Planck equation as

$$\frac{\partial C}{\partial t} = - \sum_{i=1}^2 \frac{\partial}{\partial z_i} \mu_i C + \sum_{i,i'=1}^2 \frac{\partial^2}{\partial z_i \partial z_{i'}} D_{ii'} C, \quad (5.13)$$

which corresponds to the Langevin stochastic differential equation (SDE)

$$dz_i = \mu_i(\mathbf{z}) dt + \sum_{j=1}^2 \sigma_{ij}(\mathbf{z}, t) dW_j \quad \text{for } i = 1, 2, \quad (5.14)$$

where $\mathbf{z} = (v, w)$,

$$\sigma = \begin{pmatrix} \sqrt{2D_{11}} & 0 \\ 0 & \sqrt{2D_{22}} \end{pmatrix}, \quad (5.15)$$

and W_j is a Wiener process such that $\langle W_j(t) \rangle = 0$ and $\langle W_j(t) W_{j'}(t') \rangle = \delta_{jj'} \min(t, t')$. In terms of the original model parameters, we find that

$$D_{11} = \frac{1}{N} f_{\text{Na}}(v)^2 a_\infty(v) [1 - a_\infty(v)]^2$$

and

$$D_{22} = w \beta_K + (1 - w) \alpha_K(v).$$

The latter result was previously obtained by Fox and Lu [6] and the former by Keener and Newby [26]. Equation (5.14) can now be linearized about the stable rest state by letting $z_j = z_j^* + \epsilon \eta_j(t)$ where $\mu_j(\mathbf{z}^*) = 0$. Taylor expanding to $O(\epsilon)$ yields

$$d\eta_i(t) = \sum_{j=1}^2 A_{ij} \eta_j + \sum_{j=1}^2 \sigma_{ij}(\mathbf{z}^*) dW_j, \quad (5.16)$$

where A_{ij} is the Jacobian of the drift terms such that

$$A_{ij} = \left. \frac{\partial \mu_i}{\partial z_j} \right|_{\mathbf{z}^*}.$$

Finally, introducing white noise processes $\xi_j(t)$ such that $dW_j(t) = \xi_j(t) dt$ with $\langle \xi_j(t) \rangle = 0$ and $\langle \xi_j(t) \xi_{j'}(t') \rangle = \delta_{jj'} \delta(t - t')$ allows us to formally write the SDE as

$$\frac{d\eta_i(t)}{dt} = \sum_{j=1}^2 A_{ij} \eta_j + \sum_{l=1}^2 \sigma_{il}(\mathbf{z}^*) \xi_l. \quad (5.17)$$

VI. QUASICYCLES IN THE STOCHASTIC MODEL

Using our linear SDE (5.17), we can now look for oscillations in either voltage or potassium dynamics by obtaining

analytical expressions for the power spectra. Let $\tilde{\eta}_j(\omega)$ denote the Fourier transform of $\eta_j(t)$, i.e.,

$$\tilde{\eta}_j(\omega) = \int_{-\infty}^{\infty} e^{-i\omega t} \eta_j(t) dt. \quad (6.1)$$

Here we follow standard steps to derive power spectra, as in [31,32]. Taking the Fourier transform of (5.17) yields

$$\tilde{\eta}_j(\omega) = \sum_{i=1}^2 \Phi_{ij}^{-1}(\omega) \sigma_{ij} \tilde{\xi}_i(\omega), \quad (6.2)$$

where $\Phi_{ij} = -i\omega \delta_{i,j} - A_{ij}$. Recall that the power spectrum $P_i(\omega)$ is defined such that $2\pi \delta(0) P_i(\omega) = \langle |\tilde{\eta}_j(\omega)|^2 \rangle$. Using Eq. (6.2), we obtain the power spectrum for the stochastic ML model

$$P_i(\omega) = \sum_j \sum_k \Phi_{ij}^{-1}(\omega) D_{jk} (\Phi_{ki}^\dagger)^{-1}(\omega), \quad (6.3)$$

where we have used $\Phi_{ij}(-\omega) = \Phi_{ji}^\dagger(\omega)$. It is worth mentioning that when comparing the analytical power spectrum to one that is generated numerically, one must take care to include a proportionality factor. This arises from the use of the discrete Fourier transform when computing numerical spectra and is equal to a time increment of Δt in the time series. A peak in the voltage power spectrum for $\omega \neq 0$ indicates that the voltage is oscillating with frequency ω .

As can be seen in Fig. 3, the spectrum of voltage when $I_{\text{app}} = 150$ in the model shows a maximum around the Hopf frequency $\omega_c = 1.51$. This means that the model exhibits subthreshold oscillations at this frequency, despite the fact that this is well below the supercritical Hopf bifurcation point. In other words, channel noise from the stochastic opening and closing of Na^+ and K^+ channels is driving subthreshold oscillations outside the deterministic regime. We also compare our analytic power spectrum against numerical estimates of the power spectrum obtained using the Gillespie algorithm [37] and find good agreement. Next we explore the range of applied current for which the membrane potential exhibits a subthreshold oscillation. With channel noise, we first see the emergence of oscillatory behavior for $I_{\text{app}} = 93$. Including channel noise from stochastic K^+ and Na^+ channels increases both the range of applied currents for which subthreshold oscillations are present and the range of frequencies of these subthreshold oscillations (Fig. 4). This analysis provides support for the claim that channel noise increases a neuron's ability to produce subthreshold oscillations, particularly for stimuli that are weak.

As we already highlighted in Sec. IV within the context of a double system-size expansion, we expect the contribution of Na^+ channel noise to be dominant. This is indeed found to be the case under our QSS approximation. The relative contribution of Na^+ versus K^+ channel noise can be quantified by looking at the magnitude of the respective diagonal terms in the diffusion matrix D (see Fig. 5). With physiological parameter values ($\epsilon \in [10^{-3}, 10^{-2}]$, $N \sim 10^3$), D_{11} , the term in the diffusion matrix affected by N and ϵ (and thus Na^+), is orders of magnitude larger than D_{22} . Therefore, in this parameter regime, Na^+ channel noise is dominant. While fixing N and ϵ we asked whether there was a physiologically plausible number of K^+ channels M that would allow for Na^+

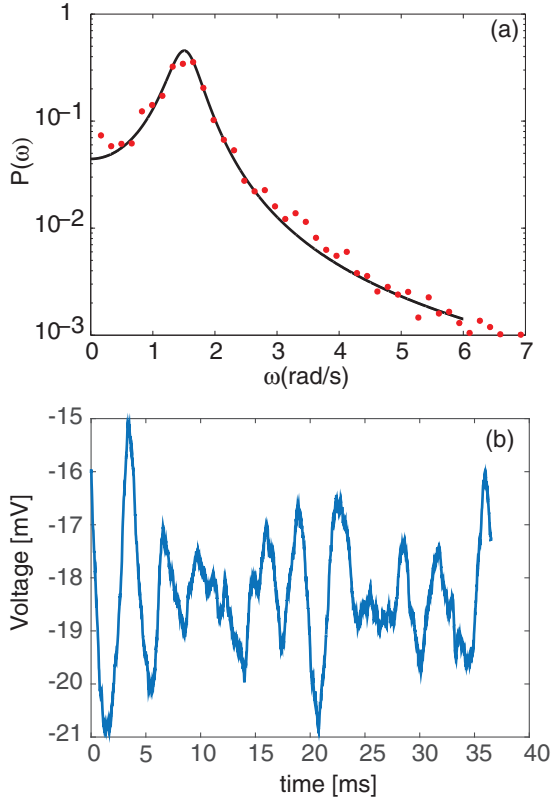


FIG. 3. (Color online) (a) Power spectrum of the voltage in the stochastic hybrid ML model for $I_{app} = 150$. The spectrum has a well-defined peak around the Hopf frequency $\omega_c = 1.51$ rad/s, indicating the presence of oscillations (quasicycles) below the supercritical Hopf bifurcation point. Filled (red) circles are from numerical simulations via the Gillespie algorithm, whereas the black solid line is the analytical prediction. The simulation values are $N = 10^3$, $M = 10^4$, and 50 trials. (b) Time domain response of voltage for a particular realization of the simulation shows STO-like behavior.

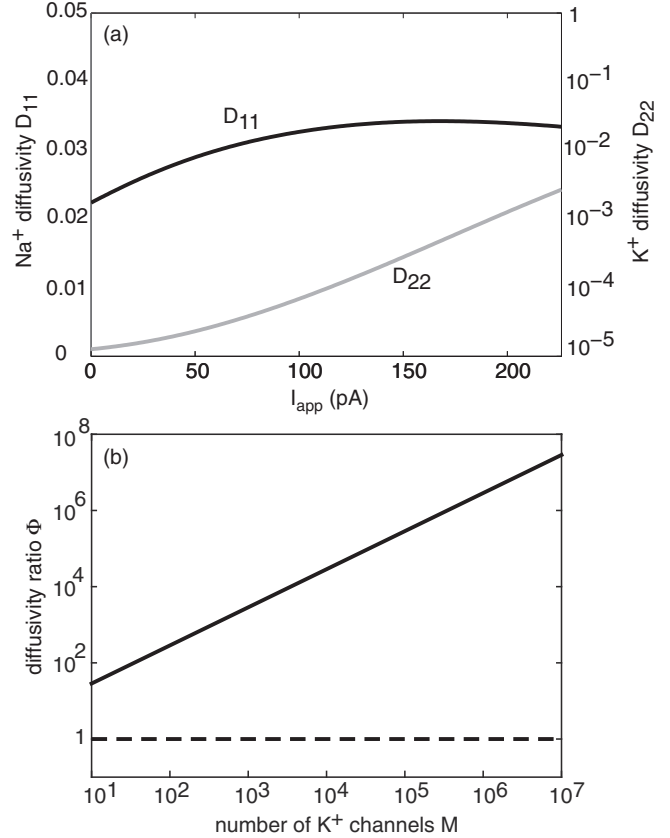


FIG. 5. Comparison of the contribution of Na⁺ and K⁺ channel noise to the diffusion term in the SDE. (a) Comparing D_{11} and D_{22} , with $N = 10^3$, $M = 10^4$, and $\epsilon = 10^{-2}$. Here D_{11} (and thus the contribution of Na⁺ channel noise) is orders of magnitude larger for all values of I_{app} . (b) Fixing $\epsilon = 10^{-2}$ and $N = 1000$, there are no values of $M > 10$ such that the magnitudes D_{11} and D_{22} are comparable, i.e., the ratio $\Phi = D_{11}/D_{22}$ is always greater than 1 (dotted black line).

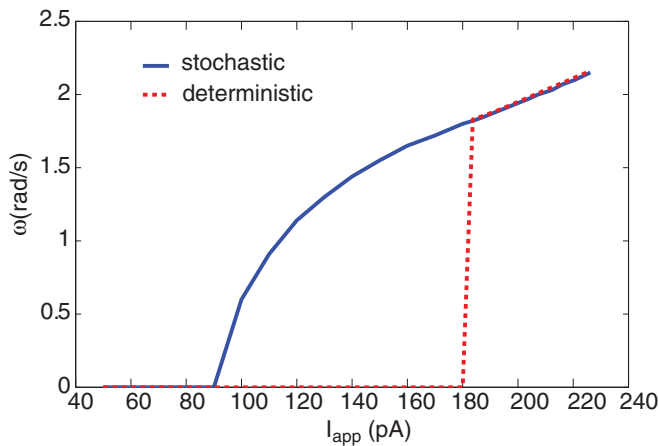


FIG. 4. (Color online) Channel noise increases the range of applied current values for which subthreshold oscillations exist. It also increases the range of frequencies that the model may produce. Frequency of oscillation ω is defined as the maximum of the power spectrum $P(\omega)$ for a given I_{app} . Here $N = 10^3$, $M = 10^4$, and $\epsilon = 10^{-3}$.

and K⁺ channel noise to have a comparable effect. As shown in Fig. 5, the neuron would have to have fewer than ten K⁺ channels for this to be the case. This leads us to the conclusion that fast Na⁺ channel dynamics are the primary source of channel noise.

Another factor that could be important is the degree of coherence of the noise-induced subthreshold oscillations as a function of applied current; only sufficiently coherent oscillations would allow for a synchronization code, for example. One measure of coherence is the so-called quality factor $Q = \omega_c/\Delta\omega$, where $\Delta\omega$ is the bandwidth of the power spectrum and ω_c is the peak. In Fig. 6 we plot Q as a function of I_{app} for three cases: Na⁺ channel noise, K⁺ channel noise, and joint channel noise. It can be seen that over a wide range of I_{app} , the system with stochastic K⁺ channels exhibits more coherent oscillations than the one with stochastic Na⁺ channels. Interestingly, the Q factor itself exhibits some form of resonance, having a sharp peak at some critical value of the applied current.

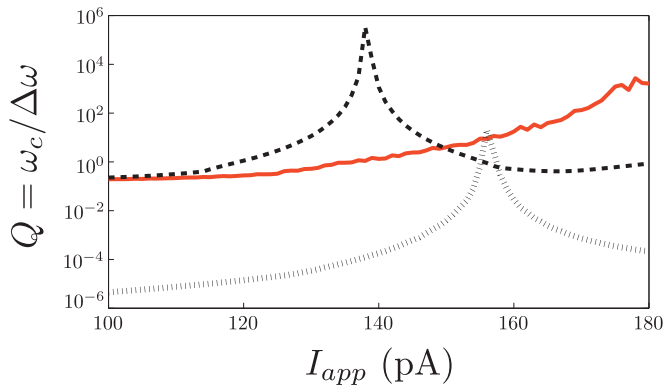


FIG. 6. (Color online) Quality factor $Q = \omega_c / \Delta\omega$ for the model with stochastic Na^+ channels only (black dashed line), stochastic K^+ channels only (gray dotted line), and both channel types stochastic (red solid line). Here ω_c is the critical value of ω , i.e., the peak of the power spectrum $P(\omega)$, and $\Delta\omega$ is the bandwidth. With K^+ channel noise, the oscillations tend to be more coherent (larger Q factor). The parameter values are the same as in Fig. 4.

VII. DISCUSSION

In conclusion, we have shown how the noise-induced formation of STOs can be modeled in terms of the emergence of quasicycles in a stochastic hybrid ML model with both persistent sodium and potassium channel noise. This is consistent with biological data that show that channel noise enables a neuron's ability to generate subthreshold oscillations and enhance signal transduction over a wide range of parameter values. From a mathematical perspective, we have shown how one can preserve the low-dimensional (planar) structure of the deterministic ML model by carrying out a QSS approximation of the stochastic sodium channel dynamics. This method for reducing the dimensionality of the Langevin equation can be applied to any stochastic hybrid system with fast kinetics.

The computational advantages of the QSS method over a diffusion approximation based on a system-size expansion become particularly significant when the complexity of the ion channel model increases. As we highlighted in Sec. II, one major simplification of the stochastic ML model is to neglect that fact that ion channels typically have a subunit

structure resulting in multiple states [25]. If these features were included, then the simple birth-death process used to describe the opening and closing of a two-state ion channel would need to be generalized to a more complicated multistate master equation. (It might be possible to obtain some simplifications by identifying invariant submanifolds of the stochastic dynamics [38].) Carrying out a system-size expansion of the resulting master equation would generate a high-dimensional Langevin equation that couples the voltage to additional variables representing the fraction of ion channels in each of the states. However, the numerical calculation of the associated diffusion matrix (or its square root) is numerically expensive. Fox and Lu [6] tackle this by approximating the multistate system in terms of uncoupled gating particles. However, such a simplification can lead to a breakdown of the diffusion approximation. More recently, a number of groups have shown that the diffusion approximation holds provided one considers coupled gating particles [11,39–41]. The QSS reduction is also a Gaussian approximation, but is based on a slow-fast decomposition rather than a system-size expansion, which eliminates the fraction of ion channels in each state as dynamical variables. Since the resulting Langevin equation is lower dimensional than in the case of the system-size expansion, one avoids the computational issues highlighted in Refs. [11,39–41]. On the other hand, the calculation of the pseudoinverse that determines the diffusion coefficient D_{11} in Eq. (5.13) could become computationally expensive as the complexity of the fast ion channel models increases.

Another possible extension of this work would be to consider the effects of noise-induced subthreshold oscillations on spontaneous action potentials (SAPs) by including a second class of nonpersistent Na^+ channels. The effects of channel noise on SAPs in excitable neuron models has recently been investigated within the context of noise-induced escape problems [1,26,27]. Diffusionlike approximations such as the system-size expansion and QSS analysis break down for such problems and one has to use alternative methods such as Wentzel-Kramers-Brillouin and large-deviation theories.

ACKNOWLEDGMENTS

P.C.B. was supported by the National Science Foundation (Grant No. DMS-1120327) and H.A.B. by the National Science Foundation (Grant No. RTG-1148230).

-
- [1] P. C. Bressloff, *Stochastic Processes in Cell Biology* (Springer, Basel, 2014).
- [2] A. A. Faisal, L. P. J. Selen, and D. M. Wolpert, *Nat. Rev. Neurosci.* **9**, 292 (2008).
- [3] J. A. White, J. T. Rubinstein, and A. R. Kay, *Trends Neurosci.* **23**, 131 (2000).
- [4] P. N. Steinmetz, A. Manwani, C. Koch, M. London, and I. Segev, *J. Comput. Neurosci.* **9**, 133 (2000).
- [5] B. Sakmann and E. Neher, *Single-Channel Recording*, 2nd ed. (Plenum, New York, 1995).
- [6] R. F. Fox and Y. N. Lu, *Phys. Rev. E* **49**, 3421 (1994).
- [7] C. C. Chow and J. A. White, *Biophys. J.* **71**, 3013 (1996).
- [8] K. Diba, H. A. Lester, and C. Koch, *J. Neurosci.* **24**, 9723 (2004).
- [9] G. A. Jacobson, K. Diba, A. Yaron-Jakobovitch, Y. Oz, C. Koch, I. Segev, and Y. Yarom, *J. Physiol.* **564**, 145 (2005).
- [10] M. H. Kole, S. Hallermann, and G. J. Stuart, *J. Neurosci.* **26**, 1677 (2006).
- [11] J. H. Goldwyn, N. S. Imennov, M. Famulare, and E. Shea-Brown, *Phys. Rev. E* **83**, 041908 (2011).
- [12] E. Schneidman, B. Freedman, and I. Segev, *Neural Comput.* **10**, 1679 (1998).
- [13] A. D. Dorval, *Neuroscientist* **12**, 442 (2006).
- [14] A. A. Faisal, J. A. White, and S. B. Laughlin, *Curr. Biol.* **15**, 1143 (2006).

- [15] X. J. Wang, *Neuroreport* **5**, 221 (1993).
- [16] A. Alonso and R. R. Llinas, *Nature (London)* **342**, 175 (1989).
- [17] R. R. Llinas, A. A. Grace, and Y. Yarom, *Proc. Natl. Acad. Sci. U.S.A.* **88**, 897 (1991).
- [18] J. A. White, R. Klink, A. Alonso, and A. R. Kay, *J. Neurophysiol.* **80**, 262 (1998).
- [19] R. Amir, C. N. Liu, J. D. Kocsis, and M. Devor, *Brain* **125**, 421 (2002).
- [20] A. Reboreda, E. Sanchez, M. Romero, and J. A. Lamas, *J. Physiol.* **551**, 191 (2003).
- [21] D. T. W. Chik, Y. Wang, and Z. D. Wang, *Phys. Rev. E* **64**, 021913 (2001).
- [22] B. Ermentrout and D. Terman, *Mathematical Foundations of Neuroscience* (Springer, New York, 2010).
- [23] C. Morris and H. Lecar, *J. Biophys.* **35**, 193 (1981).
- [24] J. A. White, T. Budde, and A. R. Kay, *Biophys. J.* **69**, 1203 (1995).
- [25] G. D. Smith, in *Modeling the Stochastic Gating of Ion Channels*, edited by C. Fall, E. S. Marland, J. M. Wagner, and J. J. Tyson (Springer, New York, 2002), Chap. 11.
- [26] J. P. Keener and J. M. Newby, *Phys. Rev. E* **84**, 011918 (2011).
- [27] J. M. Newby, P. C. Bressloff, and J. P. Keener, *Phys. Rev. Lett.* **111**, 128101 (2013).
- [28] A. D. Dorval and J. A. White, *J. Neurosci.* **25**, 10025 (2005).
- [29] U. Kummer, B. Krajnc, J. Pahle, A. K. Green, C. J. Dixon, and M. Marhl, *Biophys. J.* **89**, 1603 (2005).
- [30] A. J. McKane, J. D. Nagy, T. J. Newman, and M. O. Stefanini, *J. Stat. Phys.* **128**, 165 (2007).
- [31] R. P. Boland, T. Galla, and A. J. McKane, *J. Stat. Mech.* (2008) P09001.
- [32] P. C. Bressloff, *Phys. Rev. E* **82**, 051903 (2010).
- [33] J. Realpe-Gomez, T. Galla, and A. J. McKane, *Phys. Rev. E* **86**, 011137 (2012).
- [34] A. Juel, A. G. Darbyshire, and T. Mullin, *Proc. R. Soc. London Ser. A* **453**, 2627 (1997).
- [35] C. Gardiner, *Handbook of Stochastic Methods*, 4th ed. (Springer, Berlin, 2009).
- [36] T. G. Kurtz, *Math. Prog. Stud.* **5**, 67 (1976).
- [37] D. T. Gillespie, *J. Phys. Chem.* **81**, 2340 (1977).
- [38] B. A. Earnshaw and J. P. Keener, *SIAM J. Appl. Dyn. Syst.* **9**, 220 (2010).
- [39] D. Linaro, M. Storace, and M. Giugliano, *PLoS Comput. Biol.* **7**, e1001102 (2011).
- [40] P. Orio and D. Soudry, *PLoS ONE* **7**, e36670 (2012).
- [41] D. Pezo, D. Soudry, and P. Orio, *Front. Comput. Neurosci.* **8**, 139 (2014).